Journal of ELECTRONIC MATERIALS, Vol. 42, No. 4, 2013
DOI: 10.1007/s11664-012-2292-2

Impact of Electrical Current on the Long-Term Reliability of Fine-Pitch Ball Grid Array Packages with Sn-Ag-Cu Solder Interconnects

TAE-KYU LEE[1,2]

1.—Component Quality and Technology Group, Cisco Systems, Inc., San Jose, CA 95134, USA.
2.—e-mail: taeklee@cisco.com

The interaction between electrical current and the long-term reliability of fine-pitch ball grid array packages with Sn-3.0Ag-0.5Cu (wt.%) solder ball interconnects is investigated. In this study, 0.4-mm fine-pitch packages with 300-μm-diameter Sn-Ag-Cu solder balls are used. Electrical current was applied under various conditions to two different package substrate surface finishes to compare the effects of chemically unmixed and mixed joint structures: a Cu/SAC305/Cu structure and a NiAu/SAC305/Cu structure, respectively. To study the thermal impact on the thermal fatigue performance and long-term reliability, the samples were thermally cycled from 0°C to 100°C with and without current stressing. Based on Weibull plots, the characteristic lifetime was degraded for the mixed joint structure, but little degradation was observed for the unmixed joint structure. The microstructure evolution was observed during constant current stressing and current stressing during thermal cycling. Accelerated intermetallic precipitation depletion at the package-side interface was observed in NiAu/SAC305/Cu structures due to current stressing, which was identified as the potential reason for the degradation in the thermal cycling performance.

Key words: Pb-free solder, current stressing, isothermal aging, microstructure, NiAu surface finish, OSP surface finish

INTRODUCTION

In recent years, electronic components have begun to be incorporated into smaller, higher-functionality, higher-density packages, which require increased power within a given number of interconnections in a given area.[1–3] This trend has brought the attention of researchers to interconnects with higher electrical current flow, which ultimately causes electromigration. Electromigration in solder joint interconnects has become increasingly important as joints have decreased in size and the current densities within them have increased in magnitude.[4–9] Several failure mechanisms have been identified, several detailed studies have been conducted, and the topic is still under active investigation. The identification of potential failure modes in Cu-Sn systems is particularly important in light of the trend toward Pb-free solder systems.[10] Several factors affect the diffusion induced by electrical current flow through a solder joint. This includes not only the back-stress caused by electrical current flow but also the Joule heating from localized hot spots.[11] These can affect the overall microstructure of the solder joint and the vacancy formation and migration, among other factors. This focus on the high current density per interconnect has resulted in understanding of well-studied phenomena such as void formation and current crowding, which are crucial to determine the lifetime of solder interconnects subjected to relatively high current density stressing.[12] However, at the same time, it has become important to identify the current stressing impact of relatively low current densities on long-term solder joint stability and reliability. It is reported that electrical current can

(Received December 14, 2011; accepted September 25, 2012; published online October 27, 2012)

significantly affect mechanical behavior, such as the creep of Sn-Ag-Cu solder alloys over time when exposed to isothermal aging and *in situ* current stress.[13,14] Additionally, it is important to look into the potential degradation of the overall lifetime of the solder joint for relatively low current densities for prolonged periods of time because the impact of isothermal aging on fine-pitch electronic components is identified in earlier publications.[15,16] The potential explanation for the impact of isothermal aging was linked to localized Cu depletion, which accelerated the reliability degradation rate. Because current stressing aligned with the direction of the current is directly associated with Cu diffusion, the impact of current stressing is expected to be directly correlated to either acceleration or deceleration of the degradation of the solder joint reliability. Because it is well known that the electrical current can accelerate the Cu diffusion, it is important to identify the impact of the electrical current on the long-term reliability, which replicates the real function and performance of the component. In this study, board-level thermal cycle reliability tests have been performed on daisy-chained lead-free 0.4-mm-pitch ball grid array (BGA) components with body size of 13 mm × 13 mm. The tests were performed on two different package substrate surface finishes to compare the effects of chemically unmixed and mixed joint structures: a Cu/SAC305/Cu structure and a NiAu/SAC305/Cu structure to reveal the impact of long-term current stressing and investigate the impact of Cu migration driven by current stressing.

EXPERIMENTAL PROCEDURES

As shown in Fig. 1, the samples used in this study were 13 mm × 13 mm body size BGAs with four-row perimeter arrays and a total of 432 solder joints. The solder ball diameter was 300 μm, and they were arranged in the package with a 0.4 mm pitch, which is the distance between the mid-points of each solder ball. The composition of the solder balls used in this study was Sn-3.0Ag-0.5Cu (wt.%) (SAC305). All BGA samples had single 10.05 mm × 10.05 mm silicon die attached, and the package-side substrates had either electrolytic Ni/Au surface finish or organic surface preservative (OSP) surface finish on top of the Cu substrate. The Ni and Au layer thickness for the electrolytic Ni/Au surface finish were 5 μm and 0.1 μm, respectively, with 10% thickness variation for the Ni layer and 5% variation for the Au layer. Parts were attached to a 2.4-mm-thick 370HR printed circuit board (PCB) with glass-transition temperature (T_g) of over 170°C with organic surface preservative (OSP) surface finish on top of Cu. Sn-3.0Ag-0.5Cu (wt.%) (SAC305) solder paste was used for the board assembly reflow with typical peak temperature of 240°C and 60 s above the liquidus temperature. All components assembled on the printed circuit boards were daisy-chained. Figure 1b shows five continuous solder joints from Fig. 1a indicated in the box marked as "section A." The internal circuit was connected so that the applied current can flow from the board to the package side through each solder joint. An electrical current was applied to the samples with a constant current so that each solder joint experienced current density of 2000 A/cm^2 at room temperature and at elevated temperature of 80°C. To achieve the current density of 2000 A/cm^2, a current of 0.76 A was applied. This level of current produce Joule heating due to the Cu trace and interconnect resistivity, which needs to be carefully considered during the thermal cycling test. The correlation between the measured applied current and the temperature of the top and near the solder joint of

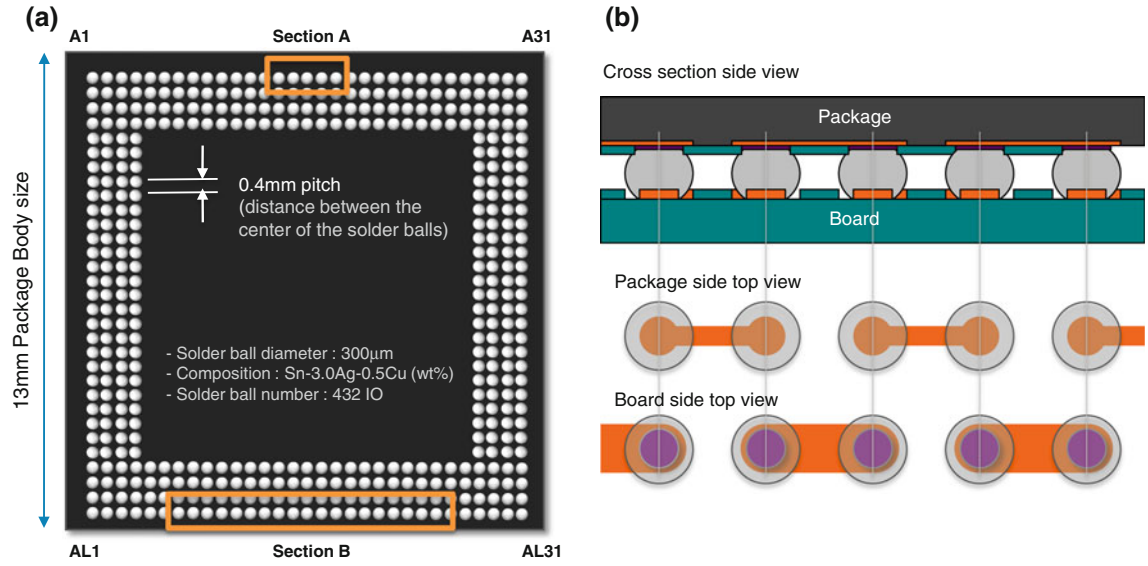

Fig. 1. Fine-pitch BGA sample configuration (a) and schematic side-view after board assembly (b).

the component can be seen in Fig. 2. With 0.76 A current stressing, the temperature of the component is increased to 33.6°C at the top of the component and 30.5°C at the board side; the temperature was measured 0.6 mm away for the corner solder joint with a 300-μm-diameter ball-tip K-type thermocouple attached to the target area with silver paste. The temperature measurement values are from the component and not from the interface of a solder joint. Since there are more detailed studies performed in earlier publications by various groups, which addressed the joint temperature in a more accurate way, this study did not further pursue the measurement at the joint. In an earlier publication on a more simplified joint structure we measured the temperature of the solder joint by the same method of attaching a thermocouple, and confirmed by infrared measurement with an IR camera as well as a finite-element computer model.[14] The joint interface temperature increased to approximately 40°C at current density of 4000 A/cm^2, and 50°C at current density of 5500 A/cm^2. To compensate the Joule heating effect, the board-level accelerated thermal cycling (ATC) test profile was adjusted to perform according to IPC-9701A in the temperature range of 0°C to 100°C, with ramp rates of 10°C/min and dwell time of 10 min. In order to have a consistent method of measuring the effect of current density on thermal fatigue life, the thermal cycle temperature profile was controlled to be consistent with and without current stressing. In order to connect multiple components with a constant current density through the duration of the test, components under test were serially connected in a single net. For each net, a DC power supply was deployed in constant current mode. Resistivity increases due to solder joint failures were recorded indirectly by voltage drop across the net. The initial resistivity values of each component were in the range of 1.3 Ω to 2.2 Ω depending on the location of the component and length of the wire. Since the 20% failure criterion is hard to identify from the voltage drop across the net, the 100 Ω failure criterion was used.

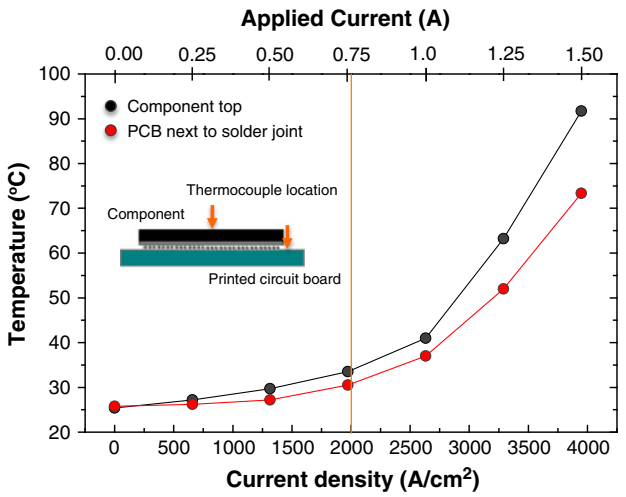

Fig. 2. Component temperature measurement with current stressing.

RESULTS AND DISCUSSION

Microstructure Evolution During Static Current Stressing

Figure 3 shows the initial microstructure right after board assembly for each surface-finished solder joint.[15] The scanning electron microscopy (SEM) images show scallop-shaped intermetallic compound (IMC) for both surface finish samples at the board-side interface (Fig. 3c, f). However, a slight difference can be identified in that larger individual unit scallop-shaped IMCs occur in the OSP surface-finished samples. For higher aspect ratios, smaller-sized scallop-shaped IMCs are observed at the OSP surface-finished board-side IMCs, and more nearly needle-shaped IMCs are mixed in the Ni/Au surface finish sample. In addition, relatively finer IMC precipitates are observed in the OSP sample compared with the Ni/Au-finished sample. It is expected that all of these differences are caused by the presence of Ni in the system, which diffuses into the system during ball attachment reflow and the board assembly reflow process.

After board assembly, samples were pretreated with various current stress conditions: current stressed with 2000 A/cm^2 at room temperature or in 80°C ambient air for 1000 h. Figure 4a and b show cross-sectional SEM images after current stressing with 2000 A/cm^2 current density for 1000 h at room temperature and at 80°C, respectively. The SEM images are presented for the first row of samples. The five solder joints are continuously located at A15-A20 (indicated in Fig. 1a, section A). Because they are connected with one daisy-chained circuit, the applied electrical current direction during the pretreatment was from the board side toward the package side in joint A15 and from the package side toward the board side in joint A16, and so on. The microstructure after 1000 h of pretreatment showed migration of the intermetallic precipitates, depending on the current direction. In Fig. 4b (joint A15), a large number of accumulated IMC precipitates are shown inside the bulk solder in which the current flow was from the board side to the package side. Compared with A15, A16 shows a relatively small number of IMC precipitate clusters in which the current flow was from the package side to the board side. The same IMC migration can be observed in joint A17 and A18. Because the package-side surface finish is electrolytic NiAu, the Ni acts as a diffusion barrier and prevents the Cu from flowing into the bulk solder. The joints that have the electrical current flow from the package to the board side show migration of the IMC toward the board side, which results in a relatively wide IMC-free solder bulk microstructure. In contrast, the joints

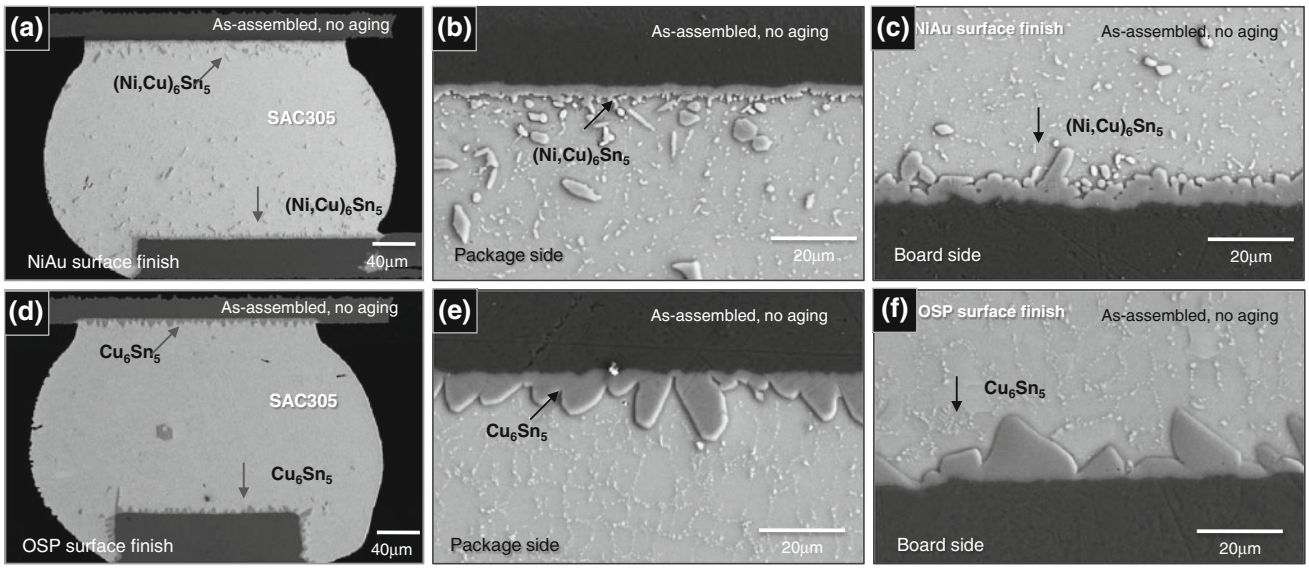

Fig. 3. SEM microstructure after board assembly (unaged): (a) overall view of the electrolytic Ni/Au surface finish joint and (b) higher magnification of the Ni/Au package-side interface and (c) board-side interface; (d) overall view of the OSP surface finish joint and (e) higher magnification of the OSP package-side interface and (f) board-side interface.[15]

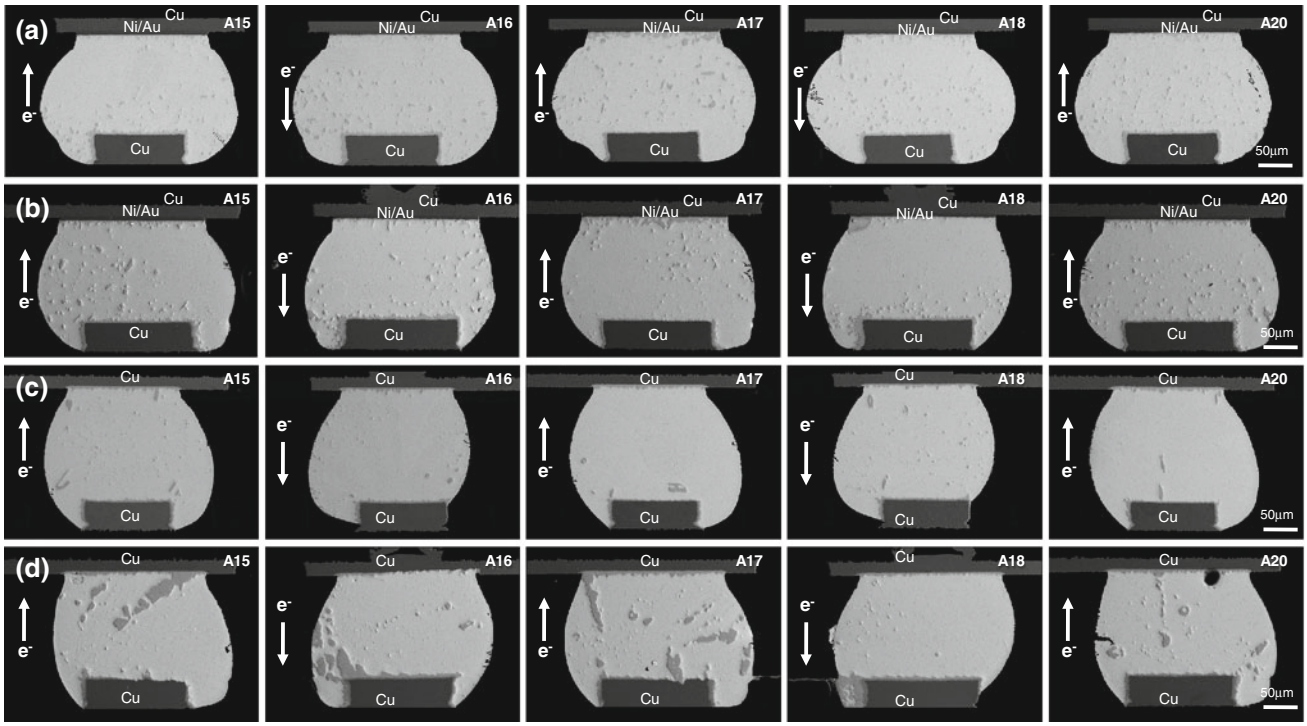

Fig. 4. SEM microstructure after current stressing with 2000 A/cm^2 current density for 1000 h at (a) room temperature, and (b) at 80°C on NiAu surface-finished samples, and (c) at room temperature, and (b) at 80°C on OSP surface-finished samples.

with the current flow from the board to the package side have more Cu diffusion from the board-side Cu pad, which results in the more IMC accumulated solder bulk microstructure observed here. Overall, it seems that the current drove the Cu from the package side toward the board side in the case of the current stress from the package to the board side. No further Cu can flow into the solder bulk on the package side due to the NiAu diffusion barrier. Compared with the joints that experienced the current flow from the package side to the board side, the joints that experienced the current stressing in the opposite direction have more Cu diffusion toward the package side if there is a sufficient Cu

supply from the board-side Cu pad. This phenomenon continued for samples that were current-stressed at high temperatures with the same current density. It is not yet clear where the Cu resides after diffusing into the region via the current flow. Most likely, with sufficient activation energy, the Cu will first reside in the Sn grain boundaries and contribute to the growth of Cu_6Sn_5 precipitates. The activation energy can be supplied by the elevated temperature. The Cu near the interface can be used to grow the interface IMC layer, which contributes to forming a Cu depletion layer near the interface, which was reported in earlier publications.[15,16] However, the exact mechanism is still not clear and is definitely a topic that should receive additional attention in the near future.

Figure 4c and d show samples with an OSP surface finish on the package side. Therefore, no diffusion barrier is present in these samples between the package side Cu pad and the solder bulk. As shown in Fig. 4c, not much microstructure change is observed. Because the current stressing is applied at room temperature, an accumulation of Ag_3Sn IMC is observed, but not much microstructure transformation at the package- and board-side Cu pad and solder bulk interface is observed. Figure 4d presents a sample that was current-stressed at 80°C. An increase of the Cu_6Sn_5 IMC inside the bulk solder is observed, especially in joint A15, A17, and A19, in which the current flows from the board to the package side. The surface of the Cu pad at the board side showed concave surfaces, which is an indication that Cu has diffused into the solder bulk. Additionally, joints A16 and A18, which experienced current stressing from the package to the board side, show active Cu diffusion into the bulk solder at the package Cu pad region. An accumulation of Cu_6Sn_5 IMC at the board-side interface is observed, which is caused by current stressing. Overall, a microstructure evolution occurred at the interface at both the package- and board-side interface IMCs, but not much microstructure transformation occurred inside the solder bulk. The sufficient source of Cu at both the package- and board-side Cu pad provided an unmixed joint structure in which less Cu gradient was built up during the current stressing.

Thermal Cycling with *In Situ* Current Stressing

Given that the Cu gradient after current stressing based on the current direction was identified, to see the impact of this Cu gradient effect due to current stressing, an accelerated thermal cycling test was applied to the samples with and without *in situ* current stressing. Figure 5 shows a Weibull plot of the results of thermal cycling on unaged NiAu and OSP surface-finished BGA samples with and without *in situ* current stressing. Twenty-four samples were tested for samples without current stressing, and 12 samples per surface finish were tested with current stressing. The first failure occurred at approximately 1200 cycles for the unaged, as-assembled conditions for both NiAu and OSP. By considering the characteristic lifetime cycle number, which is the cycle number at a 63.5% failure rate, the characteristic life cycle number for unaged, as-assembled NiAu surface finish samples without applying electrical current was 2457 cycles (Fig. 5a). With *in situ* current stressing, the characteristic lifetime cycle degraded to 1998 cycles, which is a reduction of 19% in the characteristic lifetime. Compared with the NiAu surface-finished samples, the OSP surface-finished sample thermal cycling results are shown in Fig. 5b. The characteristic lifetime cycle number without current stressing was 1793 cycles, which is lower than for the NiAu unaged, no-current-applied samples. There is a difference in the characteristic lifetime with a slightly higher cycle number for the NiAu surface finish, but the gap is relatively small. This is expected due to the presence of Ni in the solder joints in the bulk solder region near the package-side interface, which increases the initial hardness and provides more crack propagation resistance. However, with *in situ* current stressing, the lifetime characteristic cycle number increased to 1812 cycles, which is actually a 1% increase in lifetime expectancy. However, the Weibull plot in Fig. 5b showed an overlapping failure distribution, which means that those two conditions resulted in very similar lifetime expectancies. Other than the characteristic life cycle number, there is little difference between the first failures with and without current stressing for both NiAu and OSP surface-finished samples, and like the characteristic life cycle number for both surface finishes, the 1% failure cycle number for NiAu samples showed a larger cycle number degradation, from ~1500 cycles to ~900 cycles, versus a slight increase from ~1150 cycle to ~1250 cycles for OSP surface-finished samples.

Microstructure Evolution During *In Situ* Current Stressing During Thermal Cycling

One possible explanation for the different characteristic lifetime degradation values based on the surface finish can be found in the microstructure of the two different material sets for the NiAu and OSP surface-finished sample conditions. Comparing Fig. 6a and b reveals different IMC precipitation distributions and microstructure evolution after *in situ* current stressing during thermal cycling. The cross-sectional SEM images in Fig. 6a show the microstructure of solder joints A15–A19 after thermal cycling. Full cracks were observed at joints A17 and A19, in which the current was applied from the package side toward the board side. In contrast, joints A16 and A18, with the current applied from the board to the package side, showed only partial cracks or no crack propagation. This is an indication

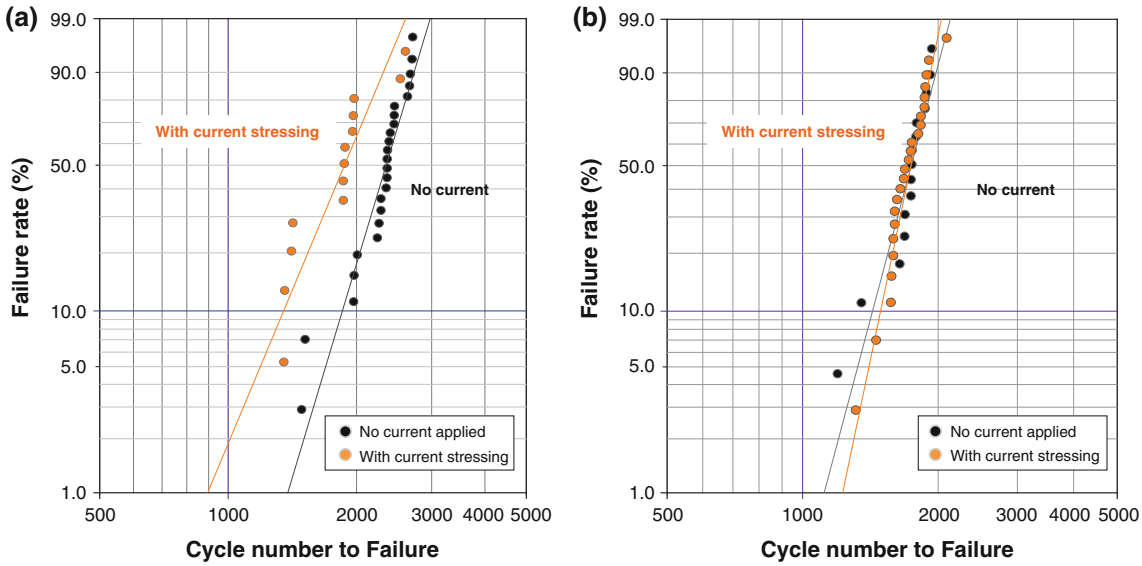

Fig. 5. Weibull plot for thermal cycling results with and without *in situ* current stressing for BGA samples: (a) NiAu surface-finished samples (b) OSP surface-finished samples.

that the fatigue crack propagation is accelerated depending on the current flow direction inside the solder joint, in this case, for NiAu surface-finished samples. However, in the case of OSP surface-finished samples, the accelerated crack propagation is not observed. As shown in Fig. 6b, the OSP surface-finished samples, after thermal cycling, exhibited a large microstructure evolution at the package- and board-side IMC interface, but no specific crack propagation dependency on current flow direction was observed. In Fig. 6b (joint A15), a thicker IMC layer developed during thermal cycling with *in situ* current stressing from the package to the board side, which was associated with Cu pad consumption at the package-side Cu interface. The same phenomenon, but in the opposite direction, occurred in joint A18, in which the current flow was from the board side toward the package side.

Figure 7 show higher-magnification SEM images of the microstructures from the areas indicated in Fig. 6. Figure 7a and e show images from the interface at the package side and the board side, wherein the current stressing was applied from the board side toward the package side. A locally IMC-depleted zone was observed near the board-side interface (Fig. 7e), and an IMC (Cu_6Sn_5) thickness growth was observed at the package-side interface. The fine Ag_3Sn IMC precipitate distribution was maintained, which is actually a different microstructure after thermal cycling without current stressing. In an earlier publication,[15] after thermal cycling, the microstructure showed IMC layer growth and depletion zone formation at the package-side interface in the case of NiAu surface-finished samples. However, as observed here in Fig. 7a, the electric current affected the Cu migration and stabilized the Ag_3Sn IMC precipitates, resulting in a strengthening mechanism, which mitigates the crack propagation shown in Fig. 6a for joints A16 and A18. Joints A16 and A18 showed that the crack propagation route was actually detoured and avoided the IMC stabilized area, resulting in crack propagation mitigation and a longer lifetime. However, when the joint experiences current stressing from the package side toward the board side, an IMC precipitate depletion zone reappears, as shown in Fig. 7b. Because the package-side surface finish is NiAu, no Cu can diffuse into the solder bulk from the package-side Cu pad, resulting in a Cu depletion zone near the interface. A similar IMC and Cu depletion due to isothermal aging was also observed in earlier test results,[15,16] which accelerated the crack propagation. An IMC thickness growth at the board side (Fig. 7f) is observed, which was caused by the Cu diffusion induced by the current flow from the package side to the board side. Combining the effect of the current stressing direction, a localized strengthening occurred at the package-side interface solder bulk area when the current flow is from the board to the package side, which mitigates the crack propagation and improves the thermal fatigue performance. In contrast, a current-induced IMC depletion occurs when the current flow is from the package side toward the board side, which accelerates the crack propagation and reduces the thermal performance of the solder joint.

The microstructures at the interface as shown by SEM for OSP surface-finished samples are compared with NiAu surface-finished samples in Fig. 7c, d and g, h. Figure 7c, g and d, h show the package-side and board-side interface from a joint that experienced a current flow from the board side to the package side and from the package side to the board side, respectively. The Cu pad interface shows

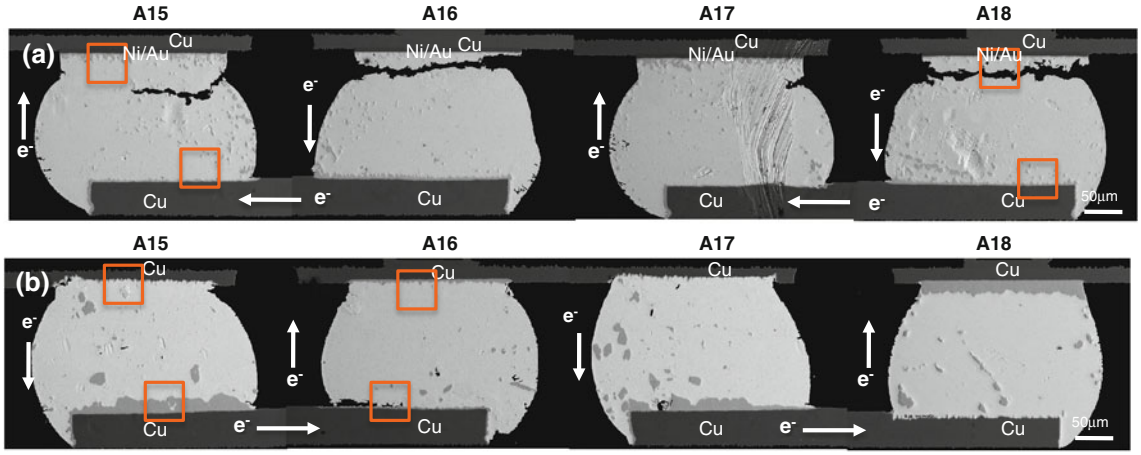

Fig. 6. SEM microstructure after *in situ* electro-current stressing during thermal cycling with 2000 A/cm^2 current density for: (a) NiAu surface-finished package samples, and (b) OSP surface-finished package samples. The electro-current direction is indicated by the arrow.

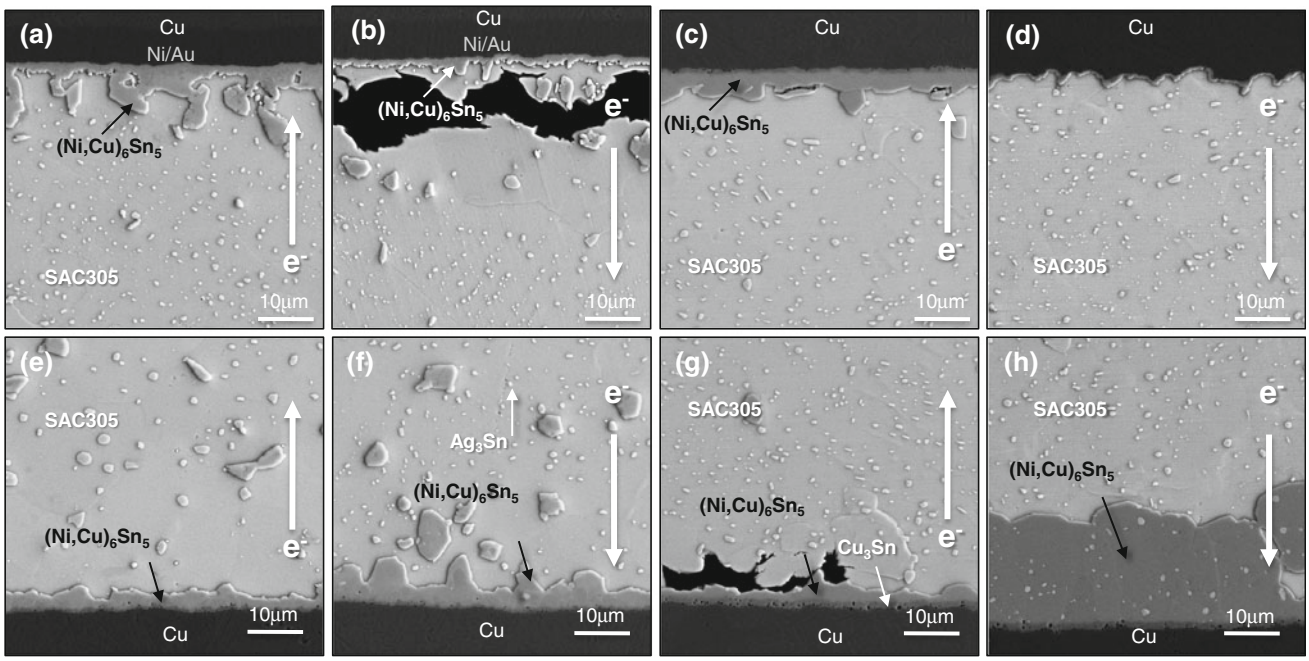

Fig. 7. SEM microstructure after *in situ* electro-current stressing during thermal cycling with 2000 A/cm^2 current density. Higher-magnification SEM microstructures from the areas indicated in Fig. 6. NiAu surface-finished package: (a, e) joint A15 and (b, f) joint A18; OSP surface-finished package: (c, g) joint A15 and (d, h) joint A16. The electro-current direction is indicated by the arrow.

Cu dissolution into the solder bulk, and an aggressive IMC thickness growth on the board side is observed. Although the microstructure evolution happened aggressively at the interface IMC, the IMC precipitates inside the solder bulk exhibited little change in their distribution. Both joints which experienced current stressing in the upward and downward direction (Fig. 7c, g and d, h) showed homogeneously distributed IMC precipitates. The thermal cycling results between the *in situ* current applied and not-applied lifetime cycle showed no differences, as shown in the Weibull plot in Fig. 5b. The homogeneously distributed IMC observed in Fig. 7c, g and d, h provides a potential explanation. Unlike the NiAu surface-finished samples, the OSP surface-finished samples have sufficient Cu sources at both the package- and board-side Cu pads. Both current flow directions ultimately affected the microstructure at the interface IMC, but with Cu entering the solder joint without difficulty, the IMC precipitates inside the solder joint maintained a homogeneous distribution because there is no Cu chemical gradient through the solder joint with the OSP surface finish. The result with little or no

impact on the characteristic lifetime during current stressing with OSP surface-finished components provided a better characteristic lifetime from a thermal cycling perspective, but at the same time, the continuous consumption of the Cu at the package and board side can also pose potential risks, which can introduce other reliability issues. Thus, stating that OSP surface-finished components are more stable than NiAu surface-finished components with *in situ* current stressing during thermal cycling is only valid if the Cu layer can sufficiently supply Cu into the solder joint system without degrading the joint structure itself.

CONCLUSIONS

The interaction between the electrical current and the long-term reliability of fine-pitch BGA packages with Sn-3.0Ag-0.5Cu (wt.%) solder ball interconnects is investigated. Electrical current was applied to fine-pitch BGA packages with 300-μm-diameter Sn-Ag-Cu solder balls. Two different package substrate surface finishes are selected to compare the effects of a chemically unmixed and mixed joint structure: the Cu/SAC305/Cu structure and NiAu/SAC305/Cu structure, respectively. Based on Weibull plots for each aging condition and surface finish type, the lifetime of the package was degraded with the NiAu/SAC305/Cu joint structure, but little degradation was observed in Cu/SAC305/Cu joint structures. Based on the current stressing direction, in a NiAu/SAC305/Cu joint structure, a localized strengthening occurred at the solder bulk area near the package-side interface when the current flow is from the board to package side, which mitigates the crack propagation and improves the thermal fatigue performance. On the other hand, a current-induced IMC depletion occurred when the current flow is from the package side toward the board side, which accelerates the crack propagation and reduced the thermal performance of the solder joint. Little impact was identified in Cu/SAC305/Cu joint structured package thermal cycling performance due to stable IMC precipitate distribution as long as the Cu layer at both package and board side can sufficiently supply the Cu into the solder joint system without degrading the joint structure.

ACKNOWLEDGEMENTS

This work was supported by the Cisco Component Quality and Technology group.

REFERENCES

1. J. Glazer, *Int. Mater. Rev.* 40, 65 (1995).
2. H.K. Kim and K.N. Tu, *Phys. Rev. B* 53, 16027 (1996).
3. J. Glazer, *J. Electron. Mater.* 23, 693 (1994).
4. J. Sanchez, L.T. McKnelly, and J.W. Morris Jr., *J. Electron. Mater.* 19, 1213 (1990).
5. C. Kim and J.W. Morris Jr., *J. Appl. Phys.* 72, 1837 (1992).
6. P.S. Ho, *J. Appl. Phys.* 41, 64 (1970).
7. K.N. Tu, *Phys. Rev. B* 49, 2030 (1994).
8. I.A. Blech and E.S. Meieran, *J. Appl. Phys.* 40, 485 (1969).
9. M. Mahadevan and R.M. Bradley, *J. Appl. Phys.* 79, 6840 (1996).
10. T.Y. Lee, K.N. Tu, and D.R. Frear, *J. Appl. Phys.* 90, 4502 (2001).
11. S.H. Chiu, T.L. Shao, C. Chen, D.J. Yao, and C.Y. Hsu, *Appl. Phys. Lett.* 88, 22110 (2006).
12. S.W. Liang, Y.W. Chang, and C. Chen, *J. Electron. Mater.* 36, 1348 (2007).
13. C. Kinney, J.W. Morris Jr., T.K. Lee, K. Liu, J. Xue, and D. Towne, *J. Electron. Mater.* 38, 221 (2009).
14. C. Kinney, T.K. Lee, K. Liu, and J.W. Morris Jr., *J. Electron. Mater.* 38, 2585 (2009).
15. T.K. Lee, H. Ma, K. Liu, and J. Xue, *J. Electron. Mater.* 39, 2564 (2010).
16. T.K. Lee, W. Xie, B. Zhou, T.R. Bieler, and K. Liu, *J. Electron. Mater.* 40, 1967 (2011).